



*Citation for published version:*

Rubio, N, Au, H, Leese, HS, Hu, S, Clancy, AJ & Shaffer, M 2017, 'Grafting from versus Grafting to Approaches for the Functionalization of Graphene Nanoplatelets with Poly(methyl methacrylate)', *Macromolecules*, vol. 50, no. 18, pp. 7070-7079. <https://doi.org/10.1021/acs.macromol.7b01047>

*DOI:*

[10.1021/acs.macromol.7b01047](https://doi.org/10.1021/acs.macromol.7b01047)

*Publication date:*

2017

*Document Version*

Peer reviewed version

[Link to publication](#)

This document is the Accepted Manuscript version of a Published Work that appeared in final form in *Macromolecules*, copyright © American Chemical Society after peer review and technical editing by the publisher. To access the final edited and published work see <https://pubs.acs.org/doi/10.1021/acs.macromol.7b01047>

## University of Bath

### General rights

Copyright and moral rights for the publications made accessible in the public portal are retained by the authors and/or other copyright owners and it is a condition of accessing publications that users recognise and abide by the legal requirements associated with these rights.

### Take down policy

If you believe that this document breaches copyright please contact us providing details, and we will remove access to the work immediately and investigate your claim.

*Grafting from* versus *grafting to* approaches  
for the functionalisation of graphene  
nanoplatelets with poly(methyl methacrylate)

Noelia Rubio,<sup>‡</sup> Heather Au,<sup>‡</sup> Hannah S. Leese, Sheng Hu, Adam J. Clancy and Milo S.  
P. Shaffer\*

Department of Chemistry, Imperial College London, London SW7 2AZ, UK.

*Keywords: graphene, functionalisation, polymer, grafting from, grafting to,  
poly(methyl methacrylate)*

Accepted: 19<sup>th</sup> August 2017

1 [\\*m.shaffer@imperial.ac.uk](mailto:m.shaffer@imperial.ac.uk)

2 ‡ Equal contribution

3 ABSTRACT Graphene nanoplatelets (GNP) were exfoliated using a non-destructive chemical  
4 reduction method and subsequently decorated with polymers using two different approaches:  
5 *grafting from* and *grafting to*. Poly(methyl methacrylate) (PMMA) with varying molecular  
6 weights was covalently attached to the GNP layers using both methods. The grafting ratios were  
7 higher (44.6% to 126.5%) for the *grafting from* approach compared to the *grafting to* approach  
8 (12.6% to 20.3%). The products were characterised using Thermogravimetric Analysis-Mass  
9 Spectrometry (TGA-MS), Raman spectroscopy, X-ray Photoelectron Spectroscopy (XPS), X-  
10 Ray Diffraction (XRD), Atomic Force Microscopy (AFM) and Transmission Electron  
11 Microscopy (TEM). The *grafting from* products showed an increase in the grafting ratio and  
12 dispersibility in acetone with increasing monomer supply; on the other hand, due to steric effects,  
13 the *grafting to* products showed lower absolute grafting ratios and a decreasing trend with  
14 increasing polymer molecular weight. The excellent dispersibility of the *grafting from*  
15 functionalised graphene, 900 µg/mL in acetone, indicates an increased compatibility with the  
16 solvent and the potential to increase graphene reinforcement performance in nanocomposite  
17 applications.

18

## 19 **Introduction**

20 Graphene related materials are proposed for bulk applications in electronic devices<sup>1</sup>,  
21 nanocomposites<sup>2-4</sup>, supercapacitors<sup>5</sup> and hydrogen storage<sup>6</sup>, amongst others. Extensive research

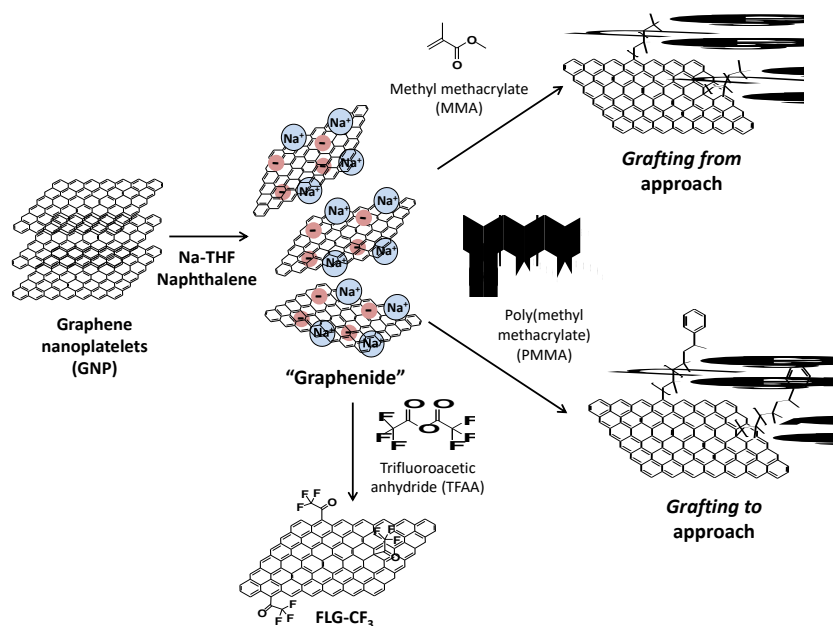
22 is underway in order to improve the compatibility of graphene with processing solvents and  
23 polymeric matrices for the preparation of composites<sup>7, 8</sup>. Covalent functionalisation provides an  
24 effective means to adjust the energetics of the surface, as well as to introduce specific steric or  
25 electrostatically stabilising moieties. Covalent approaches are more robust than non-covalent  
26 alternatives, and avoid any equilibrium with excess free surfactant. These advantages are  
27 important in many applications, for example, in the context of composites, where the aim is to  
28 enhance the strength of graphene-polymer matrix interfaces. As well as improved compatibility,  
29 covalent modification of graphene allows for the stable attachment of groups with specific  
30 functional properties (e.g. fluorescent molecules, dopants, etc.)<sup>9,10</sup>.

31 There are several methods in the literature aiming to produce single layer graphene (SLG) from a  
32 variety of starting materials (such as few-layer graphenes (FLGs), natural graphite or graphene  
33 nanoplatelets (GNPs)). These methods include liquid-phase<sup>11</sup>, mechanical<sup>12</sup> or electrochemical  
34 exfoliation<sup>13</sup>, among others. Graphite Intercalation Compounds (GICs) are established precursors  
35 to produce isolated graphene layers with minimal framework damage<sup>14-16</sup>. Exfoliated  
36 graphenides can be prepared by various routes, including potassium/liquid ammonia intercalation  
37 of graphite<sup>14</sup> and the spontaneous dissolution of potassium-based GICs in N-methyl-2-  
38 pyrrolidone (NMP)<sup>17, 18</sup>. Individual charged graphene sheets can be solvated in dry aprotic  
39 solvents, and in one recent case, transferred to water<sup>19</sup>. Yet, to stabilise the graphene in other  
40 solvents or nanocomposite materials, functional groups are often introduced. The use of  
41 covalently grafted polymers is of particular interest for the preparation of nanocomposites<sup>20</sup>.  
42 There are two main approaches to prepare polymer-modified carbon nanomaterials (CNMs):  
43 *grafting to* and *grafting from*. The *grafting to* method involves the synthesis of a polymer with a  
44 reactive end group that is attached to the surface of the CNM. This method allows explicit

45 control of the molecular weight ( $M_n$ ) and polydispersity index (PDI). Alternatively, *grafting from*  
46 involves *in situ* polymerisation of the monomer directly from the CNM. While the *grafting from*  
47 approach promises high grafting ratios, it typically requires the attachment of an initiating group  
48 prior to polymerisation<sup>21-23</sup>. *Grafting from* GO (graphite oxide) has been used to grow  
49 polystyrene and different methacrylate polymers<sup>22</sup>. These polymers were grown on the surface of  
50 GO using radical polymerisation; however, several preparation steps were involved, including  
51 the addition of an alkyne molecule to the GO followed by an azide-terminated chain transfer  
52 agent, required to initiate polymerisation. Reductive chemistry provides an alternative method  
53 that avoids the use of complex initiators. The formation of polymers in GICs was proposed  
54 several decades ago in the investigation of the influence of potassium graphite ( $KC_8$ ) in the  
55 “catalysis” of olefin polymerisation<sup>24</sup>. The formation of a “graphite-polymer-composite” was  
56 described in 1997 where the compound  $KC_{24}$  was prepared from highly oriented pyrolytic  
57 graphite (HOPG) and reacted with isoprene or styrene vapour at room temperature<sup>25</sup>. A similar  
58 technique was later used in 2006 to produce PMMA-functionalised single-walled nanotubes  
59 (SWNTs)<sup>26</sup>.

60 The dispersibility of polymer-functionalised graphene in a specific solvent should be influenced  
61 by the amount of grafted polymer and the distribution of the chains on the graphene surface but  
62 these factors are poorly understood. The comparison between *grafting from* and *grafting to*  
63 approaches has been described for the functionalisation of carbon nanotubes with polystyrene<sup>27</sup>,  
64 which showed an increase in the dispersibility of the final materials as the grafting ratio  
65 increased. A similar study was carried out with graphene oxide<sup>22</sup>; in this case, the authors  
66 reported an increase in the grafting ratio when using the *grafting from* approach. Here, we  
67 explore how the combination of reductive chemistry and different grafting approaches can

68 influence the properties of the final product, such as chain length, grafting ratio, and hence  
69 solubility. One of the objectives of this work was to maximise the ambient stability of exfoliated  
70 graphene layers in organic solvents with minimal framework damage. PMMA was used as both a  
71 classic anionic model system and a potentially relevant system in composite applications, for  
72 example to increase dispersibility in epoxies<sup>28</sup>. The second objective was to compare *grafting to*  
73 and *grafting from* approaches as a function of molecular weight to maximise exfoliation and  
74 dispersibility.



75  
76 **Scheme 1.** Grafting methods used for the functionalisation of graphene sheets with PMMA.  
77

78

79

80

## 80 **Experimental Section**

### 81 **Materials**

82 GNPs were provided by Cambridge Nanosystems UK and used without further purification. 1-  
83 Bromododecane, dodecane, copper bromide (I) (CuBr), copper bromide (II) (CuBr<sub>2</sub>), *N, N, N'*,  
84 *N'', N''*-pentamethyldiethylenetriamine (PMDETA), (1-bromoethyl)benzene, glacial acetic acid,  
85 sodium (99.95%, ingot), naphthalene (99%), poly(methyl methacrylate), trifluoroacetic  
86 anhydride and methyl methacrylate were provided by Sigma-Aldrich UK. Naphthalene was dried  
87 under vacuum overnight over phosphorus pentoxide (P<sub>2</sub>O<sub>5</sub>) before using in the glove box. THF  
88 was degassed via a freeze-pump-thaw method and dried over 20 % volume molecular sieves 3 Å  
89 before use in the glove box. Methyl methacrylate was previously purified by passing the  
90 monomer through an alumina column to remove stabilisers and then degassed using the same  
91 method as the THF. CuBr was purified by washing with glacial acetic acid, followed by 2-  
92 propanol and stored under nitrogen atmosphere.<sup>29</sup> In order to carry out the ATRP process,  
93 acetone and methyl methacrylate were distilled and stored under nitrogen. Immediately before  
94 use both monomer and solvent were purged with nitrogen for 30 min. (1-bromoethyl)benzene  
95 and PMDETA were used as received. Holey carbon films on 300 mesh copper grids used for  
96 TEM experiments were purchased from Elektron Technology UK Ltd. Aluminium oxide 90  
97 active neutral was provided by Merck UK. All gases supplied by BOC, UK.

#### 98 **Polymerisation of PMMA using ATRP**

99 In a typical experiment, CuBr (1.09 mmol, 156.06 mg) and CuBr<sub>2</sub> (0.054 mmol, 12.14 mg) were  
100 added to a Schlenk flask, equipped with a stirrer bar, which was previously evacuated and  
101 flushed with nitrogen. The flask was degassed and filled with nitrogen three times and then left  
102 under nitrogen. Subsequently, methyl methacrylate (54.26 mmol, 6 mL) and acetone (3.12 mL)  
103 were added to the flask. PMDETA (1.14 mmol, 238.8 µL) was then added to the reaction  
104 mixture and the solution was stirred until the Cu complex was formed. The mixture was

105 degassed using three freeze-pump-thaw cycles. The initiator ((1-bromoethyl)benzene) (1.05  
106 mmol, 149.4  $\mu$ L) was added after this process and the flask was placed in an oil bath and stirred  
107 at 50 °C for different periods of time (30 min, 1 h and 2 h) in order to obtain different molecular  
108 weight polymers. The reaction was then stopped by dilution with THF. The solution was filtered  
109 through a column filled with neutral aluminium oxide using THF as solvent in order to remove  
110 side products. The solvent was evaporated under reduced pressure and the polymer was  
111 precipitated in dichloromethane/diethyl ether.

112  $^1\text{H-NMR}$  ( $\text{CHCl}_3$ ,  $\delta$ , ppm): 0.77-1.092 (m, 3H,  $-\text{CH}_3$ ), 1.82 (m, 2H,  $-\text{CH}_2-$ ), 3.61 (M, 3H,  
113  $\text{COOCH}_3$ ).

114 GPC (DMF):  $M_n = 4977$  g/mol,  $\text{Đ} = 1.56$ ;  $M_n = 8039$  g/mol,  $\text{Đ} = 1.62$  and  $M_n = 9982$  g/mol,  $\text{Đ} =$   
115 1.65 for 30 minutes, 1 hour and 2 hours reaction time, respectively

### 116 **Preparation of sodium naphthalide solution**

117 In a typical experiment, 23 mg (1 mmol) of sodium and 128 mg (1 mmol) of dried naphthalene  
118 were dissolved in 10 mL of degassed anhydrous THF in a nitrogen filled glove box, and stirred  
119 using a glass stirrer for two hours forming a green sodium-naphthalene solution.

### 120 **Exfoliated graphene**

121 In a typical experiment, starting material GNP (15 mg) and a glass magnetic bar were placed in a  
122 Schlenk tube and flame-dried at 400°C under vacuum. The Schlenk tube was placed in the glove  
123 box. 1.04 mL of the sodium naphthalide solution were added to the graphene followed by 11.46  
124 mL of degassed THF (C:Na ratio used was 12, which corresponds to a sodium concentration of  
125 0.01 M).<sup>15</sup> The suspension was stirred for 24 hours. After this period of time, dry  $\text{N}_2/\text{O}_2$  80/20



126

127 was bubbled into the solution for 15 minutes, the solution was stirred for 1 day under N<sub>2</sub>/O<sub>2</sub>  
128 80/20 vol% for oxidation of any remaining charges on the graphene<sup>15</sup>. Subsequently, the  
129 graphene was filtered through a 0.2 μm PTFE filter membrane and washed thoroughly with  
130 THF, water and ethanol.

### 131 **Functionalisation of graphene with trifluoroacetic anhydride (TFAA)**

132 In a typical experiment, starting material GNP (15 mg) and a glass magnetic bar were placed in a  
133 Schlenk tube and flame-dried at 400°C under vacuum. The Schlenk tube was placed in the glove  
134 box. 1.04 mL of the Na-naphthalene solution were added to the graphene followed by 11.46 mL  
135 of degassed THF. The suspension was stirred for 24 hours. After this period of time, the reaction  
136 was sealed and transferred outside the glove box and previously degassed TFAA (0.31 mmol,  
137 44.07 μL) were added to the reaction mixture. The solution was allowed to stir for 24 hours.  
138 After this period of time, dry N<sub>2</sub>/O<sub>2</sub> 80/20 vol% was bubbled into the solution for 15 minutes, the  
139 solution was stirred for 1 day under N<sub>2</sub>/O<sub>2</sub> 80/20 for oxidation of any remaining charges on the  
140 graphene. The graphene was then filtered through a 0.2 μm PTFE filter membrane and washed  
141 thoroughly with THF, water and ethanol.

### 142 **PMMA functionalised graphene using the *grafting from* approach**

143 In a typical experiment, starting material GNP (15 mg) and a glass magnetic bar were placed in a  
144 Schlenk tube and flame-dried at 400°C under vacuum. The Schlenk tube was placed in the glove  
145 box. 1.04 mL of the Na-naphthalene solution were added to the graphene followed by 11.46 mL  
146 of degassed THF. The suspension was stirred for 24 hours. After this period of time, the reaction

147 was sealed and transferred outside the glove box and different amounts of previously degassed  
148 methyl methacrylate (1.56 mmol, 162  $\mu$ L ( $M_n = 800$  g/mol), 3.12 mmol, 337  $\mu$ L ( $M_n = 1000$   
149 g/mol), 6.24 mmol, 674  $\mu$ L ( $M_n = 1400$  g/mol), 9.36 mmol, 1.035 mL ( $M_n = 2300$  g/mol)) were  
150 added to the reaction mixture. The solution was allowed to stir for 24 hours. After this period of  
151 time, dry N<sub>2</sub>/O<sub>2</sub> 80/20 vol% was bubbled into the solution for 15 minutes, the solution was  
152 stirred for 1 day under N<sub>2</sub>/O<sub>2</sub> 80/20 for oxidation of any remaining charges on the graphene. The  
153 graphene was then filtered through a 0.2  $\mu$ m PTFE filter membrane and washed thoroughly with  
154 THF, acetone, water and ethanol.

#### 155 **PMMA functionalised graphene using *grafting to* approach**

156 In a typical experiment, starting material GNP (15 mg) and a glass magnetic bar were placed in a  
157 Schlenk tube and flame-dried at 400°C under vacuum. The Schlenk tube was placed in the glove  
158 box. 1.04 mL of the Na-naphthalene solution (1:1 in THF) were added to the graphene followed  
159 by 11.46 mL of degassed THF. The suspension was stirred for 24 hours. After this period of  
160 time, different amounts of brominated PMMA (0.104 mmol, 520 mg ( $M_n = 5000$  g/mol), 0.104  
161 mmol, 832 mg ( $M_n = 8000$  g/mol), 0.104 mmol, 1.04 g ( $M_n = 10000$  g/mol)) were added to the  
162 reaction mixture. The solution was allowed to stir for 24 hours. After this period of time, dry  
163 N<sub>2</sub>/O<sub>2</sub> 80/20 was bubbled into the solution for 15 minutes, the solution was stirred for 1 day  
164 under N<sub>2</sub>/O<sub>2</sub> 80/20 vol% for oxidation of any remaining charges on the graphene. The graphene  
165 was then filtered through a 0.2  $\mu$ m PTFE filter membrane and washed thoroughly with THF,  
166 acetone, water and ethanol.

#### 167 **Measurements**

168 TGA was performed using a METTLER Toledo TGA-DSC 1 integrated with a Hiden HPR-20  
169 QIC EGA mass spectrometer under a N<sub>2</sub> atmosphere. Samples were held at 100°C for 30 min  
170 under N<sub>2</sub> flow of 60 ml/min, then ramped at 10°C/min to 800°C. XRD measurements were  
171 carried out using dried powder samples. Data were processed using Polymer Labs Cirrus  
172 software. These samples were loaded onto zero-background XRD sample holders. The  
173 measurement was recorded at a scan rate of 0.108°/s with the Cu K $\alpha$  (1.542 Å) line using a  
174 PANalytical X'Pert PRO diffractometer. Polymer M<sub>n</sub> were assessed using a Polymer Labs GPC  
175 50 system with two PL-gel 5  $\mu$  columns. Samples were eluted with dimethylformamide (DMF)  
176 with 1% triethylamine (TEA) and 1% acetic acid. The instrument was calibrated to PMMA  
177 standards. All XPS spectra were recorded using a K-alpha<sup>+</sup> XPS spectrometer equipped with a  
178 MXR3 Al K $\alpha$  monochromated X-ray source (h $\nu$  = 1486.6 eV). X-ray gun power was set to 72 W  
179 (6 mA and 12 kV). Charge compensation was achieved using the FG03 flood gun using a  
180 combination of low energy electrons and the ion flood source. Argon etching of the samples was  
181 done using the standard EX06 Argon ion source using 500 V accelerating voltage and 1  $\mu$ A ion  
182 gun current. Survey scans were acquired using 200 eV pass energy, 1 eV step size and 100 ms  
183 (50 ms x 2 scans) dwell times. All high resolution spectra (C1s, and O1s) were acquired using 20  
184 eV pass energy, 0.1 eV step size and 1 second (50ms x 20 scans = 1000 ms) dwell times.  
185 Samples were prepared by pressing the sample onto double side sticky carbon based tape.  
186 Pressure during the measurement of XPS spectra was  $\leq 1 \times 10^{-8}$  mbar. Thermo Advantage  
187 software was used for data interpretation. Casa XPS software (version 2.3.16) was used to  
188 process the data. The quantification analysis was carried out after subtracting the baseline using  
189 the Shirley or two point linear background type. Peaks were fitted using GL(30) lineshapes; a  
190 combination of Gaussian (70%) and Lorentzian (30%). All XPS spectra were charge corrected

191 by referencing the fitted contribution of C-C graphitic like carbon in the C1s signal 284.5 eV.  
192 UV-vis-NIR absorption spectra were measured using a Perkin Elmer Lambda 950 UV-vis  
193 spectrometer in the range of wavelengths between 800 and 400 nm. A quartz cuvette with 1 cm  
194 pathlength was used for these measurements. Raman spectra of powder samples were measured  
195 using a Renishaw in Via confocal Raman spectrometer equipped with a 532 nm excitation laser  
196 source; mapping measurements were carried out using the Streamline mode (between 500 – 1000  
197 spectra over at least 3 different areas). Samples were prepared by drop casting graphene  
198 dispersions on a glass slide. The exposure time was 10 s with a laser intensity of 3.2 mW and  
199 grating 1800 l/mm. Data were analysed using Wire 4.1 and OriginPro 9. The D peak was fitted  
200 by one Gaussian function, and the G and 2D peaks were fitted using a mixture of Lorentz and  
201 Gaussian functions. Tapping-mode atomic force microscopy (AFM) measurements were taken  
202 using Bruker MultiMode 8 AFM. Samples for AFM were prepared by drop-casting dilute  
203 dispersed-graphene chloroform solutions on silica substrates. <sup>1</sup>H-NMR measurements were  
204 carried out using a Bruker NM 400 spectrometer operating at 9.4 T. Samples were dissolved in  
205 Deuterated chloroform (CDCl<sub>3</sub>) and all spectra were recorded with 16 scans. All chemical shifts  
206 ( $\delta$ ) are given in ppm, where the residual CHCl<sub>3</sub> peak was used as an internal reference ( $\delta = 7.28$   
207 ppm). TEM was carried out using a JEOL2100Plus TEM at 200 kV operating voltage. One drop  
208 of the graphene solution in acetone (100  $\mu$ g/mL) was deposited on a TEM grid and allowed to  
209 evaporate at room temperature. The TEM grid was subsequently kept under vacuum overnight  
210 before the measurement. The measurements of adsorption and desorption isotherms of nitrogen  
211 at 77 K were carried out on 20 mg-50 mg of FLG using a Micromeritics ASAP 2010 apparatus.  
212 Specific surface areas were calculated according to the Brunauer, Emmett and Teller (BET)

213 equation from the adsorption isotherms in the relative pressure range of 0.05 p/p<sub>0</sub>–0.20 p/p<sub>0</sub>.  
214 Prior to analysis, the samples were degassed with continuous N<sub>2</sub> flow at 100 °C for 12 hours.

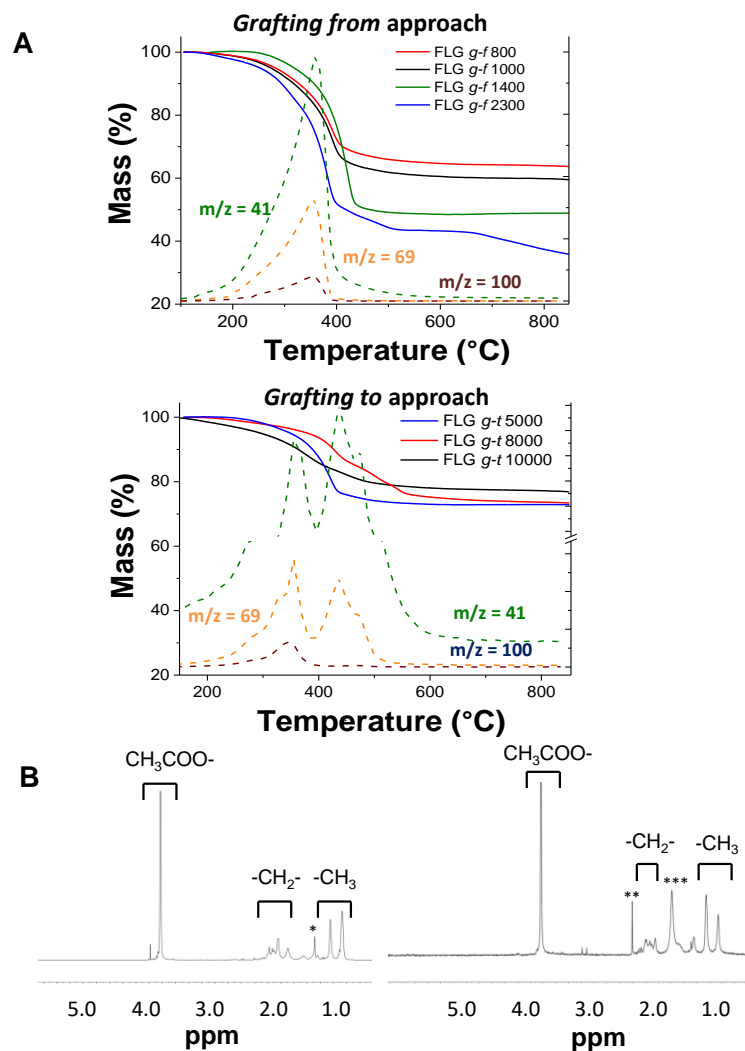
215

## 216 **Results and discussion**

217 The selected starting material was a type of GNP grown by chemical vapour deposition (CVD);  
218 it provides a relatively crystalline framework by a simple one step synthesis, whilst offering high  
219 exfoliation yields in subsequent reactions. The exfoliation of the GNP starting material was  
220 carried out using a standard methodology developed for grafting short alkyl groups<sup>15, 30</sup>: sodium  
221 and naphthalene were used as the reducing agent and transfer reagent (**Scheme 1**), respectively.  
222 Tetrahydrofuran (THF) was used as the solvent due to its ability to coordinate sodium ions<sup>31</sup>.  
223 PMMA was grafted from the graphenide by adding methyl methacrylate (MMA) monomer to the  
224 chemically reduced graphene solution. GNP was exfoliated into FLG using a C/sodium ratio of  
225 12 reported previously<sup>15</sup>, based on an optimum value found to balance the need to charge the  
226 graphenide with the tendency for charge condensation. Sodium/MMA ratios of 1:15, 1:30, 1:60  
227 and 1:90 were used in order to grow polymers of different molecular weights. The resulting  
228 GNP-PMMA products were characterised using TGA-MS under nitrogen. The GNP starting  
229 material shows a small mass loss (2.8 wt%) in the range from 100 °C to 800 °C (**Figure S1A**),  
230 probably due to the decomposition of organic impurities or oxygen functionalities, while the  
231 exfoliated sample (Na-reduced FLG) shows a mass loss (13.8 wt%) related to the presence of  
232 THF molecules in the sample (m/z = 41, **Figure S1B**). TGA-MS of PMMA-grafted FLG  
233 samples prepared using the *grafting from* approach (**Figure 1A** top panel) show the expected  
234 PMMA fragments (m/z = 69 and m/z = 100) evolved in the same temperature range on which

235 pure PMMA homopolymer fully decomposes (**Figure S3**). However, the  $m/z = 41$  peak indicates  
236 the presence of some solvent molecules within the graphene layers after the reaction, suggesting  
237 the formation of stage-1 Na-THF-GICs complexes<sup>15, 31</sup>. In order to quantify the ratio of trapped  
238 solvent and grafted PMMA on the graphene layers, the relative mass fractions of each  
239 component were estimated from the MS peaks (**Figure S2** and **Table S1** for more details).  
240 Controls were prepared by mixing either MMA or PMMA-Br ( $M_n \sim 5000$  g/mol) with quenched  
241 Na-reduced FLG (ESI); in both cases, TGA-MS after work-up (**Figure S6A-B**) showed no  
242 MMA-related signals, ruling out physisorption of either monomer or polymer. Grafting ratio is  
243 defined as the weight percentage of covalently attached polymer relative to the graphitic carbon.  
244 High grafting ratios were obtained using the *grafting from* approach (44.6% - 126.5%, **Table 1**).  
245 There are actually a number of active sites which are expected to be determined by the number  
246 of charges and is only a fraction of the total charge introduced<sup>32, 33</sup>. In order to estimate the  
247 number of active sites initiating the polymerisation, the graphenide was functionalised with  
248 trifluoroacetic anhydride (TFAA) (**Scheme 1**). This molecule is a similar size and contains a  
249 trifluoromethyl group that can be detected using TGA-MS and XPS; whilst the reactivities of  
250 TFAA and MMA may not be the identical, any variation will generate only a relative shift of  
251 otherwise consistent grafting trends. Both techniques (**Figure S5**) quantified the fluorine-  
252 containing groups grafted on the layers (one group every 149 carbon atoms from XPS  
253 calculations), and hence indicate the efficiency of the grafting reaction (**Table S2**). Raman  
254 spectroscopy (**Figure S5**) also confirmed the introduction of these functional groups. The  $M_n$  of  
255 the grafted polymer was estimated from the grafting ratio, by assuming the same density of  
256 active sites (**Table S1**). The values varied from 800 g/mol up to 2300 g/mol, increasing as  
257 expected with MMA:Na ratio.

258 Bromine-terminated PMMA polymers with different  $M_n$  were prepared for the *grafting to*  
259 approach, using Atom Transfer Radical Polymerisation (ATRP), following a previous protocol<sup>29</sup>.  
260 The polymerisation process was carried out varying the reaction times in order to obtain  
261 polymers with different  $M_n$  in the range from 5000 to 10000 g/mol. As noted above, a simple  
262 mixing control excludes possible physisorption. The negative charges on the graphene surface  
263 react with the bromine-terminated polymer (electrophile), to form the products FLG-*g-t* 5000,  
264 FLG-*g-t* 8000 and FLG-*g-t* 10000. TGA-MS analysis (**Figure 1A** bottom panel) shows typical  
265 PMMA fragments for all the grafted samples ( $m/z = 69$  and  $m/z = 100$ ). Mass loss values were  
266 extracted from the TGA graphs taking into account the amount of trapped solvent (**Table 1**).  
267 Grafting ratio decreases as the  $M_n$  of the grafted polymer increases (from 20.3% down to 12.6%,  
268 for FLG-*g-t* 5000 and FLG-*g-t* 10000, respectively), likely due to increased steric hindrance as  
269 discussed.



270  
 271 **Figure 1.** Characterisation of PMMA-grafted GNP. (A) TGA-MS of the PMMA-grafted GNP  
 272 using *grafting from* (top panel) and *grafting to* approaches (bottom panel). MS fragments  
 273 correspond to  $\text{CH}_2=\text{CH-CH}_2^+$  ( $m/z = 41$ ),  $\text{CH}_2=\text{C}=\text{C-O-CH}_3^+$  ( $m/z = 69$ ) and  $\text{CH}_2=\text{CH-CO-O-}$   
 274  $\text{CH}_3^+$  ( $m/z = 100$ ). (B)  $^1\text{H-NMR}$  spectra of commercial PMMA polymer (left panel) and FLG-*g-f*  
 275 1400 (right panel).\*, \*\* and \*\*\* indicate the presence of residual tetrahydrofuran, acetone and  
 276 water, respectively.

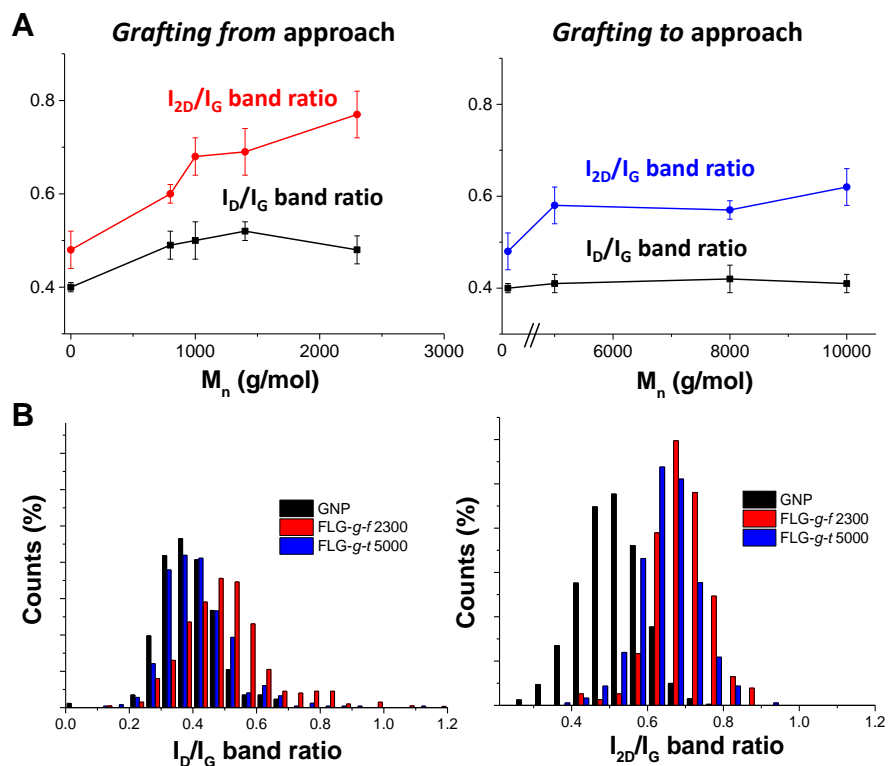
277 The  $^1\text{H-NMR}$  spectrum of commercial PMMA shows the typical signals from the polymer  
 278 (**Figure 1B** left panel). The peak at 3.6 ppm corresponds to the protons from  $\text{COOCH}_3$  in each



279 MMA unit. The peaks observed at 0.89 ppm and 1.09 ppm correspond to the CH<sub>3</sub> groups, while  
280 the peaks at 1.57 ppm are attributed to the CH<sub>2</sub> groups. These peaks can be observed in the  
281 spectrum from FLG-*g-f* 1400 (**Figure 1B** right panel), confirming the presence of polymer on the  
282 graphene layers. Polymer signals were also observed for the sample FLG-*g-f* 2300 (**Figure S7**);  
283 however, these signals were very weak for the sample FLG-*g-f* 1000, probably due to the lower  
284 polymer content and hence, dispersibility (see below). Similarly, measurable NMR peaks were  
285 weaker for the *grafting to* samples.

286 Raman spectroscopy provided quantitative data about the ratios of the D and G bands and 2D  
287 and G bands obtained from statistical mapping experiments ( $I_D/I_G$  and  $I_{2D}/I_G$  respectively)  
288 (**Figure 2**). Mean  $I_D/I_G$  values of  $0.52 \pm 0.02$  for the *grafting from* approach showed an increase  
289 compared to the GNP starting material ( $I_D/I_G$   $0.40 \pm 0.02$ , **Figure S8A**), suggesting an increase in  
290 the number of sp<sup>3</sup> atoms due to the presence of grafting sites after the polymerisation process.  
291 The much lower  $I_D/I_G$  values of  $0.42 \pm 0.03$  displayed by the *grafting to* products are not  
292 significantly greater than the Na-reduced control sample. This result is not surprising since the  
293 grafting density for the *grafting to* approach is an order of magnitude lower compared to the  
294 *grafting from* approach (**Table 1**), due to the steric bulk of the polymers. The ratio of the 2D  
295 band and G band ( $I_{2D}/I_G$ ) averages  $0.49 \pm 0.03$  for GNP starting material; an increase in this ratio  
296 indicates the presence of a higher proportion of SLG in the sample. A value of  $I_{2D}/I_G$  up to  $0.59 \pm$   
297  $0.04$  was observed for the Na-reduced FLG (**Figure S8B**), suggesting an increase in the degree  
298 of exfoliation. Higher  $I_{2D}/I_G$  ratios for PMMA grafted samples indicate greater exfoliation of the  
299 graphene layers after the functionalization. This increase in the  $I_{2D}/I_G$  ratios was larger for the  
300 *grafting from* approach (up to  $0.77 \pm 0.05$ ) compared to the *grafting to* approach ( $0.62 \pm 0.02$ ).  
301 These samples show a high intensity and symmetrical 2D band, this shape suggests the existence

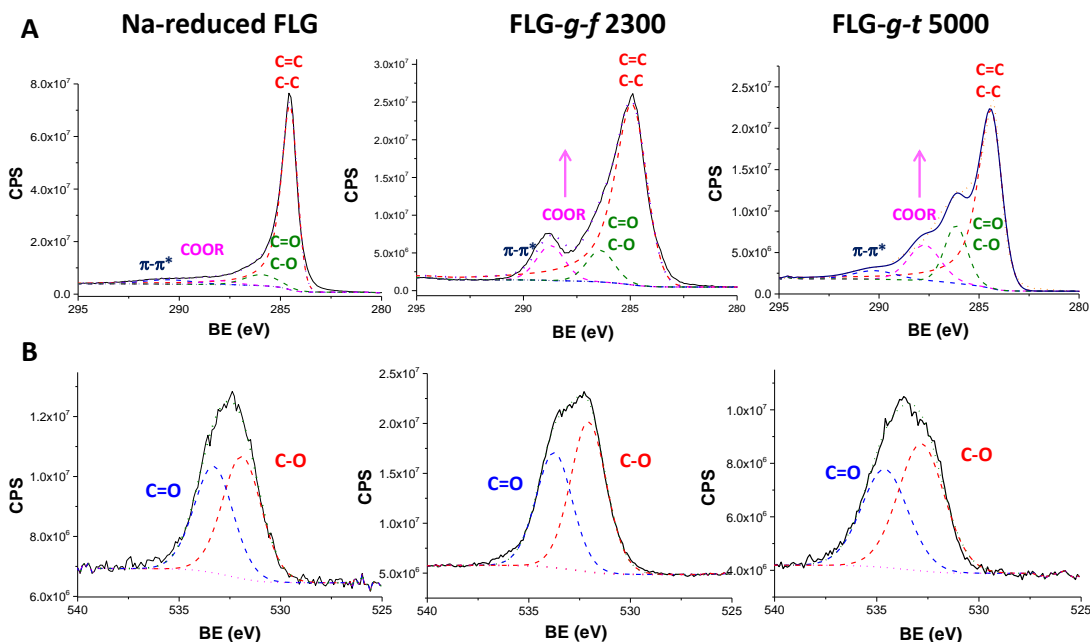
302 of single-layer and/or few layer graphene<sup>34</sup>. The full width at half maximum of the 2D band  
 303 (FWHM<sub>2D</sub>) did not change significantly between samples (**Table S5**), and is typical of  
 304 chemically exfoliated FLG<sup>35</sup>.



305  
 306 **Figure 2.** (A) Average  $I_D/I_G$  and  $I_{2D}/I_G$  ratios of FLG-PMMA obtained using *grafting from* and  
 307 *grafting to* approaches and (B)  $I_D/I_G$  and  $I_{2D}/I_G$  histograms of FLG-g-f 2300 and FLG-f-t 5000  
 308 representative samples of both approaches.

309 C1s XPS spectra of Na-reduced FLG, FLG-g-f 2800 and FLG-g-t 5000 samples (**Figure 3A**)  
 310 were deconvoluted into different bands: C=C and C-C (284.5 eV), C-O and C=O (286.4 eV),  
 311 COOR (288.7 eV) and the  $\pi$ - $\pi^*$  transition (290.7 eV) (See **Table 1** for quantitative data of all the  
 312 samples). Similar components are observed for Na-reduced FLG and for the GNP starting  
 313 material (**Figure S9**), suggesting that the exfoliation process does not itself introduce a large

314 number of additional oxygen functionalities on the graphene layers. The slight increase in the  
315 absolute amount of oxygen after the exfoliation process (from 4% to 5%) could be due to the  
316 presence of trapped solvent within the layers (**Table 1**). On the other hand, when carrying out the  
317 reaction using the *grafting from* and *grafting to* approaches, a significant increase in the COO-  
318 band appears, together with a broadening of the C=C/C-C band due to an increase in the number  
319 of C-C bonds and a higher contribution from the C=O band. The oxygen and carbon atomic  
320 percentages change very significantly after introducing the different polymers (**Table 1**). FLG-g-  
321 *f*2300 has an oxygen content of 23.5% while FLG-g-*t* 5000 sample shows a lower value of  
322 9.58%, consistent with a lower degree of functionalisation for the *grafting to* approach. The  
323 grafting density (expressed as number of graphene carbon atoms per polymer chain) obtained  
324 from XPS values is in good agreement with the results obtained from TGA values, after  
325 subtracting the excess solvent still trapped within the graphene layers (**Table 1**). For the samples  
326 obtained using the *grafting from* approach, the grafting density found from XPS varied between  
327 150 and 340, which is close to the value obtained from TGA calculations (one functional group  
328 every 149 carbon atoms). The low sodium content found in the samples ( $0.11\% \pm 0.02\%$ )  
329 indicates that the majority of the metal used for the exfoliation was removed by washing.  
330 Deconvolution of the O1s spectrum (**Figure 3B**) results in two different peaks, O-C (532.05 eV)  
331 and O=C (533.4 eV), related to PMMA, which are similar for the grafted samples.

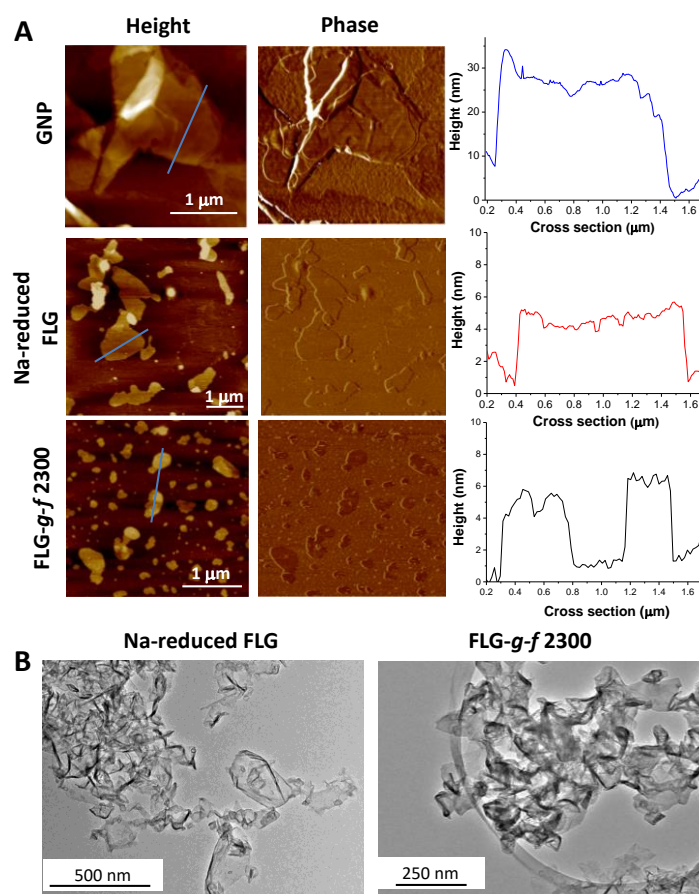


332

333 **Figure 3.** Deconvoluted XPS spectra of the (A) C1s and (B) O1s regions obtained from Na-  
 334 reduced FLG (left panels), FLG-*g-f* 2300 (middle panels) and FLG-*g-t* 5000 (right panels). These  
 335 samples were chosen as representative examples of both grafting approaches.

336 XRD measurements provide information about the interlayer distance ( $d$ ) using Bragg's law and  
 337 the number of stacked layers ( $N$ ) using the Scherrer equation<sup>36</sup>. X-ray diffractograms (**Figure**  
 338 **S10**) of the different graphene-polymer samples show the typical graphite (002) peak at a  $2\theta$   
 339 value of  $26.2^\circ$ . The weak diffraction pattern of the GNP starting material (**Figure S10**, left panel)  
 340 suggests that the graphene layers of the initial material are partially exfoliated. After the  
 341 polymerisation process, a broadening of the (002) peak is observed for all samples, indicating  
 342 successful further exfoliation of the FLG material<sup>37</sup>. The average number of layers was 41 for the  
 343 GNP starting material (**Table S6**) and 16 for the Na-reduced FLG. After functionalisation with  
 344 PMMA, the number of layers per stack decreased to an average of 6 and 9 layers for the *grafting*  
 345 *from* and *grafting to* method, respectively.

346 The morphology and degree of exfoliation of the FLG-PMMA were assessed using Atomic  
347 Force Microscopy (AFM) and Transmission Electron Microscopy (TEM) (**Figure 4**). AFM  
348 images of GNP starting material show agglomerated flakes with heights between  $20.6 \pm 5.5$  nm,  
349 corresponding to an average of 61 layers. Na-reduced FLG shows a lateral size of  $639.9$  nm  $\pm$   
350  $171.4$  nm. The presence of few-layer graphene in this sample indicates successful exfoliation of  
351 the starting material (average height:  $4.4$  nm  $\pm$   $0.61$  nm). FLG-*g-f* 2300 shows a better degree of  
352 exfoliation, the average height in this case is  $3.1$  nm  $\pm$   $0.4$  nm, in good agreement with the results  
353 obtained from XRD measurements; the average number of layers significantly decreased after  
354 functionalisation with PMMA.



355  
356 **Figure 4.** AFM images (A) of GNP starting material, Na-reduced FLG and FLG-*g-f* 2300. TEM  
357 images (B) Na-reduced FLG and FLG-*g-f* 2300.

358 **Table 1.** Summary of grafting analysis data for FLG-PMMA samples

Sample	Grafting ratio (%)	Dispersibility (mg/mL)	Grafting density <sup>a</sup>	Grafting density <sup>b</sup>	C (%) <sup>b</sup>	O (%) <sup>b</sup>	Surface concentration of grafted PMMA ( $\mu\text{mol m}^{-2}$ ) <sup>a</sup>	PMMA separation <i>D</i> (nm)	<i>R<sub>F</sub></i> (nm)
GNP	-	3.8	-	-	95.9	3.91	-	-	-
Na-reduced FLG	-	530	-	-	94.3	5.22	-	-	-
FLG- <i>g-f</i> 800	44.6	720	149	278	89.7	9.9	0.85	1.6	1.8
FLG- <i>g-f</i> 1000	55.6	760	149	334	89.2	10.1	0.80	1.6	2.1
FLG- <i>g-f</i> 1400	79.1	875	149	151	79.6	20.2	0.65	1.8	2.6
FLG- <i>g-f</i> 2300	126.5	920	149	208	75.6	23.5	0.50	2.1	5.0
FLG- <i>g-t</i> 5000	20.3	670	2055	1869	89.7	10.0	0.07	5.5	5.8
FLG- <i>g-t</i> 8000	15.1	650	4421	4390	90.9	9.0	0.03	8.0	7.7
FLG- <i>g-t</i> 10000	12.6	710	6615	5490	91.6	8.2	0.02	9.5	8.8

<sup>a</sup> Values obtained from TGA calculations. <sup>b</sup> Values obtained from XPS calculations.

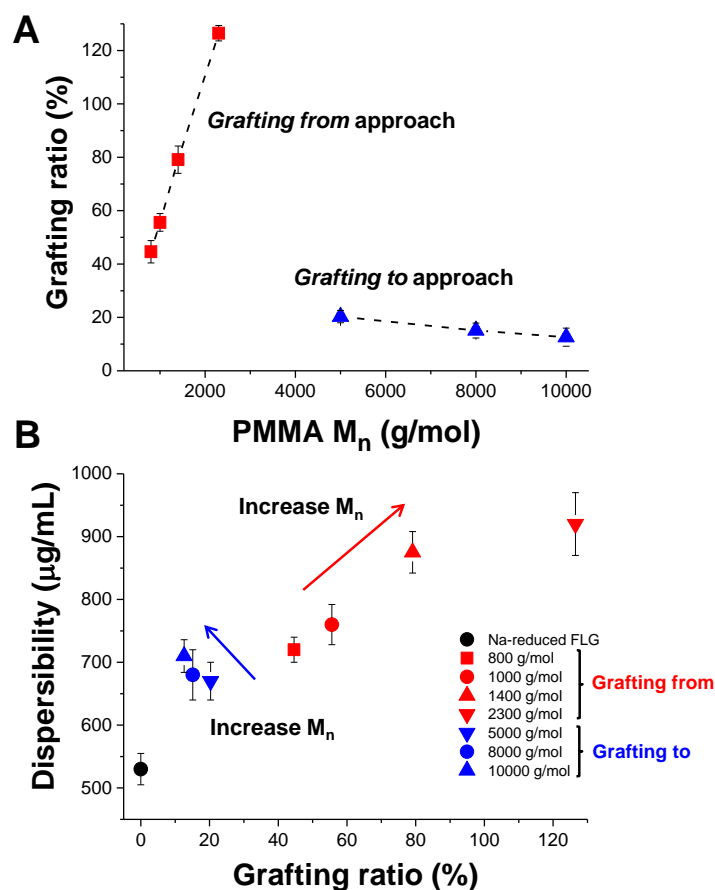
359

360 TEM images (**Figure 4B**) of Na-reduced FLG and FLG-*g-f* 2800 show a similar morphology to  
 361 the starting material (**Figure S11**), suggesting that the exfoliation/functionalisation procedure did  
 362 not damage the graphene sheets. The lateral sizes for individual graphene sheets are in the range  
 363 between 200 and 500 nm, with no significant differences observed after functionalisation.

364 Overall, the TGA-MS and XPS data indicate that PMMA polymer was successfully introduced  
 365 on the graphene surface by both *grafting from* and *grafting to* methods. Both the grafting ratio  
 366 and the grafting density were higher for the *graft from* reactions (**Table 1**). Raman and XRD data  
 367 suggest that a much greater degree of exfoliation was achieved by the *grafting from* method,  
 368 which is also supported by AFM observations.

369 The grafting ratio trend of the *grafting from* products shows an increase from 44.6% (FLG-*g-f*  
 370 1100) up to 126.5% (FLG-*g-f* 2300) as the  $M_n$  increases (**Figure 5A**); a similar trend was  
 371 reported, for the functionalisation of carbon nanotubes with polystyrene grown by ATRP<sup>27</sup>.  
 372 However, the estimated  $M_n$  values obtained for the FLG-*g-f* products were lower than reported

373 for the ring opening polymerisation of caprolactam on oxidised carbon nanotubes<sup>38</sup> (estimated  
374 1280 - 8480 g/mol). On the other hand, the *grafting to* products show the opposite trend in  
375 grafting ratios, compared to the *grafting from* approach (**Figure 5A**), most likely due to steric  
376 hindrance. Once a polymer chain grafts on the graphene surface, its volume occludes a large area  
377 of that surface, preventing grafting of another chain nearby. The grafting ratio of polystyrene-  
378 grafted to SWNTs was also reported to decrease with  $M_n$ <sup>39</sup>. For each of the FLG products, the  
379 surface concentration of grafted polymer and average PMMA chain separation,  $D$ , were  
380 estimated using the Na-reduced FLG specific surface area ( $420.08 \text{ m}^2/\text{g} \pm 4.51 \text{ m}^2/\text{g}$ ) (**Table 1**  
381 and **Table S5**)<sup>30</sup>. The conformation of the grafted PMMA polymer can be predicted from the  
382 average separation,  $D$ , between grafting sites. The estimated spacings ranged between 1.6 and  
383 2.1 nm for the *grafting from* products; this value is below the theoretical values of the Flory  
384 radius (obtained using  $R_F = M^{3/5}a$ , where  $a$  is the repeat length and  $M$  the number of monomers  
385 per chain)<sup>40</sup> for all the samples. According to de Gennes' model<sup>40</sup>, this trend suggests that the  
386 polymers must therefore grow in a brush-like fashion. Adjusting the estimates to account for the  
387 observed degree of exfoliation does not change the expected conformation (see ESI for more  
388 information). The *grafting to* approach shows  $D$  values in the range between 5.5 nm and 9.5 nm  
389 for polymer chains between 5000 and 10000 g/mol. These values are similar to or larger than the  
390 calculated  $R_F$  values (between 5.8 nm and 8.8 nm), suggesting that the polymer follows a  
391 mushroom regime in this case, where the polymer chains coil. These changes in regime are  
392 consistent with the grafting ratio trends and the proposed mechanisms.



393  
 394 **Figure 5.** Grafting density and dispersibility plots of PMMA grafted FLG using the *grafting*  
 395 *from* and *grafting to* approaches.

396 The dispersibility of PMMA-grafted FLG in acetone was quantified using UV-vis spectroscopy.  
 397 A known mass was sonicated in acetone for five minutes, allowed to sediment overnight, and the  
 398 supernatant concentrations measured using the extinction coefficient<sup>11</sup> of graphene in solution  
 399 ( $\alpha_{660} = 2460 \text{ L/g m}$ ). The dispersibility of GNP starting material was low ( $3.8 \text{ }\mu\text{g/ml}$ ) (**Figure**  
 400 **S12**) but increased remarkably for Na-reduced FLG ( $530 \text{ }\mu\text{g/ml}$ ) and polymer modified  
 401 graphene, by 250 times for FLG-*g-f* 1400 ( $920 \text{ }\mu\text{g/ml}$ ) and 170 times for FLG-*g-t* 5000 ( $650$   
 402  $\mu\text{g/ml}$ ). The trend according to the grafting ratios shows an increase in the dispersibility of the  
 403 material as the grafting ratio increases for the *grafting from* approach (**Figure 5** bottom panel).



404 On the other hand, the dispersibility behaviour remained the same for the different materials  
405 obtained from the *grafting to* approach. These values are higher than values reported in the  
406 literature for reduced-GO-PMMA with different  $M_n$  polymers attached to the graphene layers,  
407 150  $\mu\text{g/ml}$  and 140  $\mu\text{g/ml}$  for graphene-PMMA *g-f* 10000 and graphene-PMMA *g-t* 5000,  
408 respectively,<sup>22</sup> with grafting ratios of 49.3% and 50.7%, respectively. Improved grafting ratio  
409 and dispersibility results in the present study are very promising for the incorporation of PMMA-  
410 grafted FLG into different matrices.

## 411 **Conclusion**

412 In conclusion, reductive chemistry provides a route to functionalise graphene with PMMA  
413 polymers via both *grafting to* and *grafting from* approaches. Direct anionic polymerisation using  
414 graphenide as an initiator was particularly effective for grafting PMMA in situ, without the need  
415 of introducing specific initiator groups. The grafting ratio was high and systematically controlled  
416 by monomer addition. The solubility in acetone of the *grafting from* products is directly related  
417 to the  $M_n$  and grafting ratios (**Figure 5**), with an increase in the solubility when increasing  $M_n$ ;  
418 however, it is not straight forward to measure the  $M_n$  of the polymer attached on the surface of  
419 the graphene. On the other hand, while there is perfect control of the polymer  $M_n$  when using the  
420 *grafting to* approach, the solubility and grafting ratios obtained are lower compared to the  
421 *grafting from* approach. The use of reductive chemistry for *in situ* polymerization should allow  
422 the introduction of block polymers and other variants in the future. This approach should also be  
423 applicable to a range of graphitic starting materials including natural graphite, synthetic graphite  
424 or FLG. The final polymer-graphene hybrids could be used in a wide range of applications, such  
425 as sensors, as electrodes in energy storage materials, biomedical materials and in coatings for  
426 fuselages.

427 ASSOCIATED CONTENT

428 **Data statement**

429 Supporting data can be requested from the corresponding author, but may be subject to  
430 confidentiality obligations.

431 AUTHOR INFORMATION

432 **Corresponding Author**

433 \*[m.shaffer@imperial.ac.uk](mailto:m.shaffer@imperial.ac.uk)

434 **Author Contributions**

435 ‡ Equal contribution

436 **Notes**

437 The authors declare no competing financial interests.

438

439 ACKNOWLEDGMENT

440 We are grateful to Dr. Ignacio Villar-García (Imperial College London) for discussions in  
441 interpreting XPS spectra. Funding from Engineering and Physical Sciences Research Council  
442 (EPSRC/EP/K016792/1 and EP/K01658X/1) is also acknowledged. We are also grateful to  
443 Catharina Paukner (FGV Cambridge Nanosystems Limited) for providing the GNP starting  
444 material.

445

446

447

- 449 1. Zhang, J. S.; Chen, Y.; Wang, X. C. Two-dimensional covalent carbon nitride  
450 nanosheets: synthesis, functionalization, and applications. *Energ Environ Sci* **2015**, 8 (11), 3092-  
451 3108 DOI: 10.1039/c5ee01895a.
- 452 2. Wang, F. Z.; Drzal, L. T.; Qin, Y.; Huang, Z. X. Mechanical properties and thermal  
453 conductivity of graphene nanoplatelet/epoxy composites. *J Mater Sci* **2015**, 50 (3), 1082-1093  
454 DOI: 10.1007/s10853-014-8665-6.
- 455 3. Das, B.; Eswar Prasad, K.; Ramamurty, U.; Rao, C. N. Nano-indentation studies on  
456 polymer matrix composites reinforced by few-layer graphene. *Nanotechnology* **2009**, 20 (12),  
457 125705 DOI: 10.1088/0957-4484/20/12/125705.
- 458 4. Jung, H.; Yu, S.; Bae, N. S.; Cho, S. M.; Kim, R. H.; Cho, S. H.; Hwang, I.; Jeong, B.;  
459 Ryu, J. S.; Hwang, J.; Hong, S. M.; Koo, C. M.; Park, C. High through-plane thermal conduction  
460 of graphene nanoflake filled polymer composites melt-processed in an L-shape kinked tube. *ACS*  
461 *applied materials & interfaces* **2015**, 7 (28), 15256-62 DOI: 10.1021/acsami.5b02681.
- 462 5. Liu, C. G.; Yu, Z. N.; Neff, D.; Zhamu, A.; Jang, B. Z. Graphene-Based Supercapacitor  
463 with an Ultrahigh Energy Density. *Nano Lett* **2010**, 10 (12), 4863-4868 DOI:  
464 10.1021/nl102661q.
- 465 6. Tozzini, V.; Pellegrini, V. Prospects for hydrogen storage in graphene. *Phys Chem Chem*  
466 *Phys* **2013**, 15 (1), 80-89 DOI: 10.1039/c2cp42538f.
- 467 7. Ahmadi-Moghadam, B.; Sharafimasooleh, M.; Shadlou, S.; Taheri, F. Effect of  
468 functionalization of graphene nanoplatelets on the mechanical response of graphene/epoxy  
469 composites. *Mater Design* **2015**, 66, 142-149 DOI: 10.1016/j.matdes.2014.10.047.
- 470 8. Tang, L. C.; Wan, Y. J.; Yan, D.; Pei, Y. B.; Zhao, L.; Li, Y. B.; Wu, L. B.; Jiang, J. X.;  
471 Lai, G. Q. The effect of graphene dispersion on the mechanical properties of graphene/epoxy  
472 composites. *Carbon* **2013**, 60, 16-27 DOI: 10.1016/j.carbon.2013.03.050.
- 473 9. Gatti, T.; Vicentini, N.; Mba, M.; Menna, E. Organic Functionalized Carbon  
474 Nanostructures for Functional Polymer-Based Nanocomposites. *Eur J Org Chem* **2016**, (6),  
475 1071-1090 DOI: 10.1002/ejoc.201501411.
- 476 10. Liu, J. W.; Ye, Y. S.; Xue, Y.; Xie, X. L.; Mai, Y. W. Recent Advances in Covalent  
477 Functionalization of Carbon Nanomaterials with Polymers: Strategies and Perspectives. *J Polym*  
478 *Sci Pol Chem* **2017**, 55 (4), 622-631 DOI: 10.1002/pola.28426.
- 479 11. Hernandez, Y.; Nicolosi, V.; Lotya, M.; Blighe, F. M.; Sun, Z. Y.; De, S.; McGovern, I.  
480 T.; Holland, B.; Byrne, M.; Gun'ko, Y. K.; Boland, J. J.; Niraj, P.; Duesberg, G.; Krishnamurthy,  
481 S.; Goodhue, R.; Hutchison, J.; Scardaci, V.; Ferrari, A. C.; Coleman, J. N. High-yield  
482 production of graphene by liquid-phase exfoliation of graphite. *Nat Nanotechnol* **2008**, 3 (9),  
483 563-568 DOI: 10.1038/nnano.2008.215.
- 484 12. Leon, V.; Rodriguez, A. M.; Prieto, P.; Prato, M.; Vazquez, E. Exfoliation of Graphite  
485 with Triazine Derivatives under Ball-Milling Conditions: Preparation of Few-Layer Graphene  
486 via Selective Noncovalent Interactions. *Acs Nano* **2014**, 8 (1), 563-571 DOI: 10.1021/nm405148t.
- 487 13. Zhou, M.; Tang, J.; Cheng, Q.; Xu, G. J.; Cui, P.; Qin, L. C. Few-layer graphene obtained  
488 by electrochemical exfoliation of graphite cathode. *Chem Phys Lett* **2013**, 572, 61-65 DOI:  
489 10.1016/j.cplett.2013.04.013.
- 490 14. Milner, E. M.; Skipper, N. T.; Howard, C. A.; Shaffer, M. S. P.; Buckley, D. J.; Rahnejat,  
491 K. A.; Cullen, P. L.; Heenan, R. K.; Lindner, P.; Schweins, R. Structure and Morphology of

492 Charged Graphene Platelets in Solution by Small-Angle Neutron Scattering. *J Am Chem Soc*  
493 **2012**, 134 (20), 8302-8305 DOI: 10.1021/ja211869u.

494 15. Morishita, T.; Clancy, A. J.; Shaffer, M. S. P. Optimised exfoliation conditions enhance  
495 isolation and solubility of grafted graphenes from graphite intercalation compounds. *J Mater*  
496 *Chem A* **2014**, 2 (36), 15022-15028 DOI: 10.1039/c4ta02349h.

497 16. Penicaud, A.; Drummond, C. Deconstructing Graphite: Graphenide Solutions. *Accounts*  
498 *Chem Res* **2013**, 46 (1), 129-137.

499 17. Valles, C.; Drummond, C.; Saadaoui, H.; Furtado, C. A.; He, M.; Roubeau, O.; Ortolani,  
500 L.; Monthieux, M.; Penicaud, A. Solutions of Negatively Charged Graphene Sheets and  
501 Ribbons. *J Am Chem Soc* **2008**, 130 (47), 15802-+ DOI: 10.1021/ja808001a.

502 18. Catheline, A.; Valles, C.; Drummond, C.; Ortolani, L.; Morandi, V.; Marcaccio, M.;  
503 Iurlo, M.; Paolucci, F.; Penicaud, A. Graphene solutions. *Chem Commun* **2011**, 47 (19), 5470-  
504 5472 DOI: 10.1039/c1cc11100k.

505 19. Bepete, G.; Anglaret, E.; Ortolani, L.; Morandi, V.; Huang, K.; Penicaud, A.;  
506 Drummond, C. Surfactant-free single-layer graphene in water. *Nat Chem* **2017**, 9 (4), 347-352  
507 DOI: 10.1038/Nchem.2669.

508 20. Raji, A. R. O.; Varadhachary, T.; Nan, K. W.; Wang, T.; Lin, J.; Ji, Y. S.; Genorio, B.;  
509 Zhu, Y.; Kittrell, C.; Tour, J. M. Composites of Graphene Nanoribbon Stacks and Epoxy for  
510 Joule Heating and Deicing of Surfaces. *ACS applied materials & interfaces* **2016**, 8 (5), 3551-  
511 3556 DOI: 10.1021/acsami.5b11131.

512 21. Fang, M.; Wang, K. G.; Lu, H. B.; Yang, Y. L.; Nutt, S. Single-layer graphene  
513 nanosheets with controlled grafting of polymer chains. *J Mater Chem* **2010**, 20 (10), 1982-1992  
514 DOI: 10.1039/b919078c.

515 22. Ye, Y. S.; Chen, Y. N.; Wang, J. S.; Rick, J.; Huang, Y. J.; Chang, F. C.; Hwang, B. J.  
516 Versatile Grafting Approaches to Functionalizing Individually Dispersed Graphene Nanosheets  
517 Using RAFT Polymerization and Click Chemistry. *Chem Mater* **2012**, 24 (15), 2987-2997 DOI:  
518 10.1021/cm301345r.

519 23. Choi, J. H.; Oh, S. B.; Chang, J. H.; Kim, I.; Ha, C. S.; Kim, B. G.; Han, J. H.; Joo, S.  
520 W.; Kim, G. H.; Paik, H. J. Graft polymerization of styrene from single-walled carbon nanotube  
521 using atom transfer radical polymerization. *Polym Bull* **2005**, 55 (3), 173-179 DOI:  
522 10.1007/s00289-005-0426-x.

523 24. Podall, H. F., W.E.; Giraitis, A.P. Catalytic Graphite Inclusion Compounds. I. Potassium  
524 Graphite as a Polymerization Catalyst. *The Journal of Organic Chemistry* **1958**, 23 (1), 82-85.

525 25. Shioyama, H. Polymerization of isoprene and styrene in the interlayer spacing of  
526 graphite. *Carbon* **1997**, 35 (10-11), 1664-1665 DOI: Doi 10.1016/S0008-6223(97)82797-2.

527 26. Liang, F.; Beach, J. M.; Kobashi, K.; Sadana, A. K.; Vega-Cantu, Y. I.; Tour, J. M.;  
528 Billups, W. E. In situ polymerization initiated by single-walled carbon nanotube salts. *Chem*  
529 *Mater* **2006**, 18 (20), 4764-4767 DOI: 10.1021/cm0607536.

530 27. Qin, S. H.; Qin, D. Q.; Ford, W. T.; Resasco, D. E.; Herrera, J. E. Functionalization of  
531 single-walled carbon nanotubes with polystyrene via grafting to and grafting from methods.  
532 *Macromolecules* **2004**, 37 (3), 752-757 DOI: 10.1021/ma035214q.

533 28. Gomez, C. M.; Bucknall, C. B. Blends of Poly(Methyl Methacrylate) with Epoxy-Resin  
534 and an Aliphatic Amine Hardener. *Polymer* **1993**, 34 (10), 2111-2117 DOI: Doi 10.1016/0032-  
535 3861(93)90737-U.

- 536 29. Sarbu, T.; Lin, K. Y.; Ell, J.; Siegwart, D. J.; Spanswick, J.; Matyjaszewski, K.  
537 Polystyrene with designed molecular weight distribution by atom transfer radical coupling.  
538 *Macromolecules* **2004**, 37 (9), 3120-3127 DOI: 10.1021/ma035901h.
- 539 30. Leese, H. S.; Govada, L.; Saridakis, E.; Khurshid, S.; Menzel, R.; Morishita, T.; Clancy,  
540 A. J.; White, E. R.; Chayen, N. E.; Shaffer, M. S. P. Reductively PEGylated carbon  
541 nanomaterials and their use to nucleate 3D protein crystals: a comparison of dimensionality.  
542 *Chemical Science* **2016**, DOI: 10.1039/C5SC03595C.
- 543 31. Inagaki, M.; Tanaike, O. Host Effect on the Formation of Sodium-Tetrahydrofuran-  
544 Graphite Intercalation Compounds. *Synthetic Met* **1995**, 73 (1), 77-81 DOI: Doi 10.1016/0379-  
545 6779(95)03300-9.
- 546 32. Hodge, S. A.; Tay, H. H.; Anthony, D. B.; Menzel, R.; Buckley, D. J.; Cullen, P. L.;  
547 Skipper, N. T.; Howard, C. A.; Shaffer, M. S. P. Probing the charging mechanisms of carbon  
548 nanomaterial polyelectrolytes. *Faraday Discuss* **2014**, 172, 311-325 DOI: 10.1039/c4fd00043a.
- 549 33. Schafer, R. A.; Dasler, D.; Mundloch, U.; Hauke, F.; Hirsch, A. Basic Insights into  
550 Tunable Graphene Hydrogenation. *J Am Chem Soc* **2016**, 138 (5), 1647-1652 DOI:  
551 10.1021/jacs.5b11994.
- 552 34. Ferrari, A. C.; Meyer, J. C.; Scardaci, V.; Casiraghi, C.; Lazzeri, M.; Mauri, F.; Piscanec,  
553 S.; Jiang, D.; Novoselov, K. S.; Roth, S.; Geim, A. K. Raman spectrum of graphene and  
554 graphene layers. *Phys Rev Lett* **2006**, 97 (18), DOI: Artn 18740110.1103/Physrevlett.97.187401.
- 555 35. Graf, D.; Molitor, F.; Ensslin, K.; Stampfer, C.; Jungen, A.; Hierold, C.; Wirtz, L.  
556 Spatially resolved raman spectroscopy of single- and few-layer graphene. *Nano Lett* **2007**, 7 (2),  
557 238-242 DOI: 10.1021/nl061702a.
- 558 36. Saikia, B. K.; Boruah, R. K.; Gogoi, P. K. A X-ray diffraction analysis on graphene  
559 layers of Assam coal. *J Chem Sci* **2009**, 121 (1), 103-106.
- 560 37. Fujimoto, H. Theoretical X-ray scattering intensity of carbons with turbostratic stacking  
561 and AB stacking structures. *Carbon* **2003**, 41 (8), 1585-1592 DOI: 10.1016/S0008-  
562 6223(03)00116-7.
- 563 38. Zeng, H. L.; Gao, C.; Yan, D. Y. Poly(epsilon-caprolactone)-functionalized carbon  
564 nanotubes and their biodegradation properties. *Adv Funct Mater* **2006**, 16 (6), 812-818 DOI:  
565 10.1002/adfm.200500607.
- 566 39. Chadwick, R. C.; Khan, U.; Coleman, J. N.; Adronov, A. Polymer Grafting to Single-  
567 Walled Carbon Nanotubes: Effect of Chain Length on Solubility, Graft Density and Mechanical  
568 Properties of Macroscopic Structures. *Small* **2013**, 9 (4), 552-560 DOI: 10.1002/sml.201201683.
- 569 40. Degennes, P. G. Conformations of Polymers Attached to an Interface. *Macromolecules*  
570 **1980**, 13 (5), 1069-1075 DOI: Doi 10.1021/Ma60077a009.

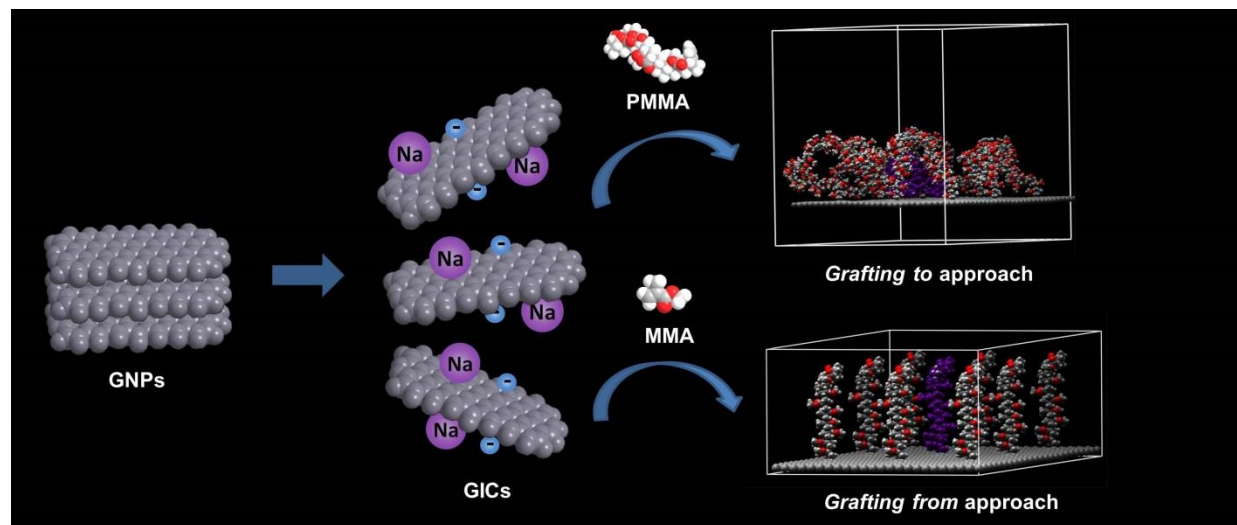
571

572

573

574

575 For table of contents use only



576

577

578